

Strong temporal variation in treefall and branchfall rates in a tropical forest is related to extreme rainfall: results from five years of monthly drone data for a 50-ha plot

Raquel Fernandes Araujo¹, Samuel Grubinger², Carlos Henrique Souza Celes¹, Robinson I. Negrón-Juárez³, Milton Garcia¹, Jonathan P. Dandois⁴, and Helene C. Muller-Landau¹

¹Center for Tropical Forest Science-Forest Global Earth Observatory, Smithsonian Tropical Research Institute, Balboa, Ancon, PO Box 0843-03092, Panama

²Department of Forest Resources Management, University of British Columbia, 2424 Main Mall, Vancouver, BC V6T 1Z4, Canada

³Climate Sciences Department, Lawrence Berkeley National Laboratory, 1 Cyclotron Road, Berkeley, CA 94720, USA

⁴Johns Hopkins University, Facilities and Real Estate, 3910 Keswick Rd. Suite N3100 Baltimore, MD 21211, USA

Correspondence to: Raquel Fernandes Araujo (araujo.raquelf@gmail.com)

Abstract. A mechanistic understanding of how tropical tree mortality responds to climate variation is urgently needed to predict how tropical forest carbon pools will respond to anthropogenic global change, which is altering the frequency and intensity of storms, droughts, and other climate extremes in tropical forests. We used five years of approximately monthly drone-acquired RGB imagery for 50 ha of mature tropical forest on Barro Colorado Island, Panama, to quantify spatial structure, temporal variation, and climate correlates of canopy disturbances, i.e., sudden and major drops in canopy height due to treefalls, branchfalls, or collapse of standing dead trees. Canopy disturbance rates varied strongly over time and were higher in the wet season, even though wind speeds were lower in the wet season. The strongest correlate of monthly variation in canopy disturbance rates was the frequency of extreme rainfall events. The size distribution of canopy disturbances was best fit by a Weibull function, and was close to a power function for sizes above 25 m². Treefalls accounted for 74 % of the total area and 52 % of the total number of canopy disturbances in treefalls and branchfalls combined. We hypothesize that extreme high rainfall is a good predictor because it is an indicator of storms having high wind speeds, as well as saturated soils that increase uprooting risk. These results demonstrate the utility of repeat drone-acquired data for quantifying forest canopy disturbance rates at fine temporal and spatial resolutions over large areas, thereby enabling robust tests of how temporal variation in disturbance relates to climate drivers. Further insights could be gained by integrating these canopy observations with high-frequency measurements of windspeed and soil moisture in mechanistic models to better evaluate proximate drivers, and with focal tree observations to quantify the links to tree mortality and woody turnover.

1 Introduction

Moist tropical forests account for 40% of the global biomass carbon stocks (Xu et al., 2021), and uncertainty regarding the future of these stocks is a major contributor to uncertainty in the future global carbon cycle (Cavaleri et al., 2015). Tropical

37 forest carbon stocks depend critically on tree mortality rates, and recent studies suggest tropical tree mortality rates may be
38 increasing due to anthropogenic global change (Brienen et al., 2015; McDowell et al., 2018). Tropical tree mortality can be caused
39 by a diversity of drivers including windthrow (Fontes et al., 2018), droughts (McDowell et al., 2018; Silva et al., 2018), fires (Silva
40 et al., 2018), lightning strikes (Yanoviak et al., 2017), and biotic agents (Fontes et al., 2018). The frequency of extreme rainfall
41 and drought events is expected to increase in tropical regions, potentially increasing associated tree mortality (IPCC, 2014; Deb et
42 al., 2018; Aubry-Kientz et al., 2019). An improved understanding of the processes of forest disturbance is critical to constrain
43 estimates of current and future carbon cycling in tropical forests under climate change (Leitold et al., 2018; Johnson et al., 2016;
44 Muller-Landau et al., 2021).

45 Despite the importance of tree mortality to forest structure and carbon turnover rates, the mechanisms underlying tree
46 mortality remain unclear (McDowell et al., 2018). A key problem is that remeasurement intervals of permanent plots average 5 or
47 more years, making it difficult to link mortality variation with particular climatic events (Phillips et al., 2010; Davies et al., 2021;
48 Arellano et al., 2019). The high rates of decomposition in tropical forests further obscure evidence of underlying mechanisms and
49 risk factors (Arellano et al., 2019). The few studies that have quantified temporal variation of tree mortality at monthly and bi-
50 monthly scales using ground-based data have all found higher tree mortality in times of higher rainfall (Brokaw, 1982; Fontes et
51 al., 2018; Aleixo et al., 2019). This is consistent with the understanding that many trees die in treefalls, which are proximately
52 caused by trunk breakage or uprooting, and are associated with storms (Marra et al., 2014; Araujo et al., 2017; Fontes et al., 2018;
53 Negrón-Juárez et al., 2017, 2018; Esquivel-Muelbert et al., 2020). The collection of additional high temporal resolution mortality
54 data over large areas, together with high temporal resolution climatological data, can aid in linking mortality to particular climatic
55 events and thereby elucidating mortality mechanisms (Arellano et al., 2019; McMahon et al., 2019).

56 Drone-acquired imagery and digital aerial photogrammetry software now provide excellent tools for monitoring of forest
57 canopies (Araujo et al., 2020) and repeat drone flights can quantify canopy dynamics over large areas at high temporal resolution.
58 Photogrammetric analysis of simple RGB imagery enables reconstruction of the appearance and three-dimensional structure of the
59 top of the canopy at high spatial resolution (Dandois and Ellis, 2013; Araujo et al., 2020; Zahawi et al., 2015). Comparison of
60 photogrammetry products from successive drone flights allows easy detection and quantification of canopy disturbances due to
61 treefalls and branchfalls of canopy trees. Canopy trees constitute a high proportion of stems, aboveground carbon stocks and woody
62 productivity (Araujo et al., 2020), and thus information on their mortality rates is disproportionately useful to understanding forest
63 dynamics and carbon cycling. Treefalls do not necessarily result in tree mortality (trees may survive and resprout), but almost all
64 treefalls and branchfalls result in a large flux of carbon (wood) from biomass to necromass within a short time period after the
65 event, which translates to reduced woody residence time. Periods of higher canopy disturbance rates thus represent periods of
66 higher biomass turnover, and likely correlate with higher tree mortality rates. Further, even when trees do not die from a canopy
67 disturbance event, suffering crown loss or damage increases the risk of subsequent mortality (Arellano et al., 2019).

68 Monitoring canopy disturbances with drones also provides the opportunity to precisely quantify the size distributions of
69 these canopy disturbances, and to distinguish branchfalls from treefalls. Here we define a canopy disturbance as a substantial
70 decrease in canopy height in a contiguous patch of canopy occurring over one measurement interval, such as typically results from
71 a treefall or branchfall. Marvin and Asner (2016) and Dalagnol et al. (2021) referred to these as “dynamic canopy gaps.” By
72 definition, canopy disturbances reduce canopy height and thereby change light regimes for understory and neighboring trees, and
73 the magnitude of the change depends on the disturbance size in area and depth (Hubbell et al., 1999). In general, larger canopy
74 disturbances cause larger canopy gaps as traditionally measured on the ground. Previous studies have analyzed the size distributions
75 of static gaps – areas with canopy height below a threshold – for insights into forest structure, habitat niches, and disturbance

regimes (e.g., Manrubia and Solé, 1997; Lobo and Dalling, 2013, 2014; Fisher et al., 2008). Tree species respond differently to canopy gaps of different sizes, with small gaps favoring a different set of species than large gaps (Brokaw, 1985; Denslow, 1980, 1987; Dalling et al., 2004). Branchfalls, like treefalls, are important in generating canopy gaps and contributing to woody turnover, but also often go unmeasured (Marvin and Asner, 2016; Leitold et al., 2018). Quantifying tree mortality and other damage contributes to a better understanding on change of forest structure, necromass estimates and nutrient cycling.

Here, we use five years of ~monthly drone-acquired RGB imagery for a 50 ha area of mature tropical forest on Barro Colorado Island, Panama to investigate canopy dynamics at high temporal resolution. We aim to (1) quantify temporal variation in canopy disturbance rates and its relationship to climate variation; (2) characterize the size structure of canopy disturbances; and (3) evaluate the role of branchfalls in canopy dynamics. We expect that disturbance rates will be higher in the wet season than the dry season, we hypothesize disturbance rates will increase with the frequency of extreme rainfall and wind events, and we compare the correlations of various rainfall and wind statistics with temporal variation in disturbance rates. To characterize the size structure of canopy disturbances, we quantify the size (area) distribution and evaluate whether it is best fit by power, Weibull, or exponential functions. Finally, we quantify the proportion of canopy disturbance due to branchfalls (rather than treefalls), and test whether branchfalls and treefalls exhibit similar patterns of temporal variation. Our results provide new insights into the patterns and drivers of canopy disturbance and tree mortality in this tropical forest, and illustrate the utility of drones for quantifying canopy dynamics over large areas at high temporal resolution.

2. Methods

2.1 Study site

Barro Colorado Island (BCI; 9.15° N, 79.83° W) is a 15 km² island in Central Panama, that was isolated from surrounding mainland when Lake Gatun was created as part of the construction of the Panama Canal. BCI supports tropical moist forest in the Holdridge Life Zone System (Holdridge, 1947). Annual precipitation averages approximately 2600 mm, with a pronounced dry season between January and April (a mean of about 3.5 months with < 100 mm mo⁻¹). Mean of maximum 1-day wind speeds are 8.1 m s⁻¹ and 5.8 m s⁻¹ during dry and wet seasons, respectively (https://smithsonian.figshare.com/articles/dataset/Yearly_Reports_Barro_Colorado_Island/11799111/2). Mean annual temperature is 26 °C and varies little throughout the year (Windsor, 1990). The 50 ha forest dynamics plot (1000 m x 500 m) was established on BCI in 1981 and is located in an old-growth forest (Leigh, 1999), with the exception of a small area of 1.92 ha of old secondary forest (~100 years old) in the north central part of the plot (Harms et al., 2001).

2.2 Meteorological data

Meteorological data were collected in the lab clearing and Lutz tower, approximately 1.7 km NE of the center of the 50 ha plot (https://smithsonian.figshare.com/articles/dataset/Yearly_Reports_Barro_Colorado_Island/11799111/2). Wind speed was measured using an anemometer (RM Young Wind Monitor Model 05103) installed at the top of Lutz tower, at 48 m height above ground and approximately 6 m above the top of the surrounding canopy. Wind speed measurements were made every 10 seconds, and the average, minimum and maximum values were recorded at the end of every 15-minute interval. We used the maximum

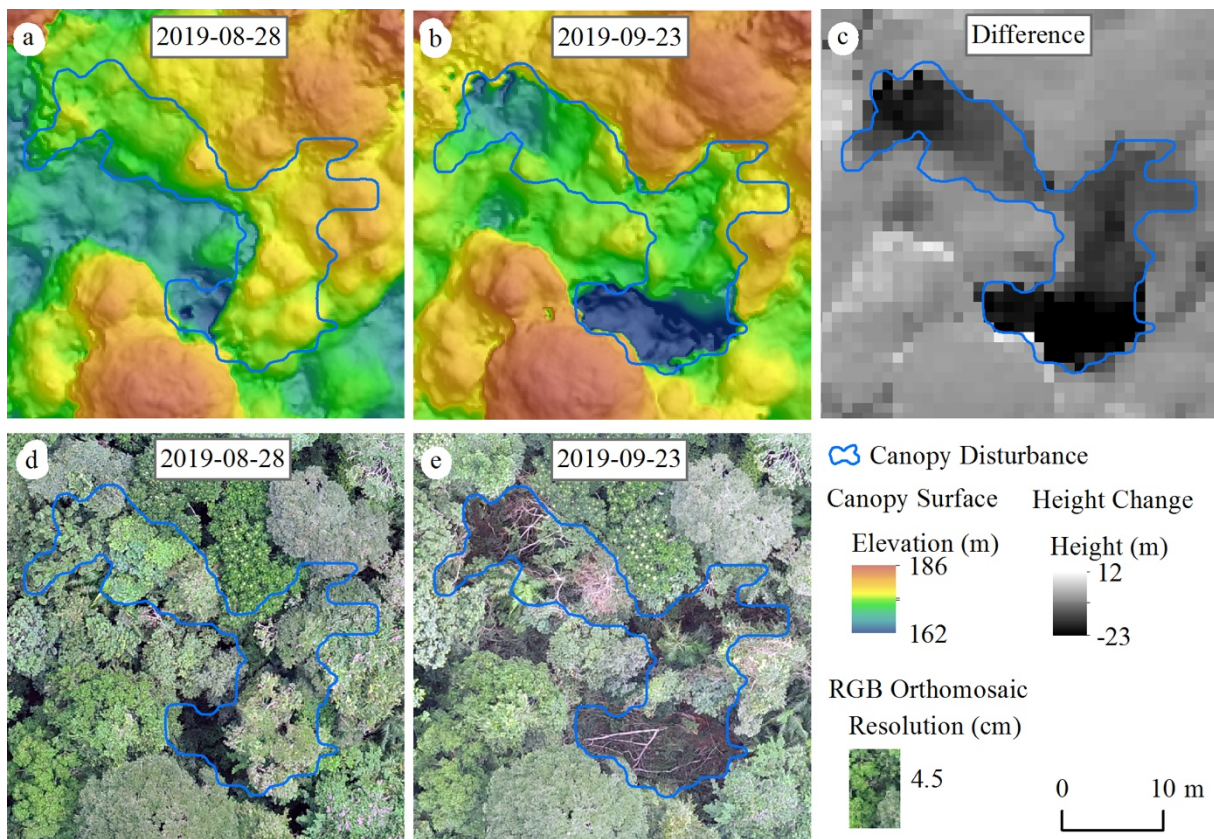
112 wind speeds for our analyses. Rainfall was measured in the lab clearing using a tipping bucket (Hydrological Services Model TB3),
113 and recorded every 5 minutes; we aggregated these data to 15-minute periods to match the temporal resolution of the wind speed
114 data. Rainfall and wind speed data are available in https://biogeodb.stri.si.edu/physical_monitoring/research/barrocolorado. The
115 meteorological record had no gaps during our study period (Fig. S1).

116

117 **2.3 Canopy disturbance identification**

118 We used approximately monthly orthomosaics and canopy surface models produced from drone-acquired imagery to
119 analyze temporal variation in canopy disturbance rates in the 50 ha forest dynamics plot between 2 October 2014 and 28 November
120 2019. RGB imagery was collected using a variety of drones and cameras over the years, with a horizontal spatial resolution of 3-
121 7 cm. Imagery for each sampling date was processed using the photogrammetry software Agisoft Metashape to obtain orthomosaics
122 and surface elevation models, which were then aligned vertically and horizontally.

123 We defined a canopy disturbance as a substantial decrease in canopy height in a contiguous patch of canopy occurring
124 over one measurement interval, such as typically results from a treefall or branchfall. We identified canopy disturbances through
125 a combination of analysis of the canopy surface model changes and visual interpretation of the orthomosaics (Fig. 1). We first
126 differenced surface elevation models for successive dates to obtain a raster of the canopy height changes for the associated interval
127 (Fig. 1, Text S1). We then pre-delineated major canopy disturbances by filtering for areas in which canopy height decreased more
128 than 10 m in contiguous areas of at least 25 m², and that had an area-to-perimeter ratio greater than 0.6. We note that 25 m² is the
129 minimum gap area used in previous studies of this site by Brokaw (1982) and Hubbell et al. (1999). The area-to-perimeter condition
130 removes artifacts associated with slight shifts in the measured positions of individual trees from one image set to another, whether
131 due to wind or alignment errors (note that this criterion involves a combination of shape and size). Finally, we systematically
132 examined 1-ha square subplots for each pair of successive dates and edited the pre-delineated polygons, removed false positives,
133 and added visible new canopy disturbances that were not previously delineated (whether because they were too small in area or in
134 canopy height drop). We also classified disturbances as being due to treefalls (a whole previously live tree fell, creating a clearly
135 visible gap on the forest floor, or the whole live crown disappeared), branchfalls (a portion of a live crown broke), or standing dead
136 trees disintegrating based on visual inspection of the orthomosaics (Fig. S2).



137

138

139

140

141

Figure 1. Canopy disturbance visualized on canopy surface models and orthomosaics calculated from photogrammetric analyses of drone imagery. (a,b) Elevation models for a portion of the study area on two successive dates, 28 August 2019 (a) and 23 September 2019 (b). (c) Difference in elevation between the two dates, with black area indicating large decrease in canopy elevation. (d,e) RGB orthomosaics of the same dates.

142

143

144

145

146

147

148

We calculated the total number and area of canopy disturbances within the BCI 50 ha plot during the 5 years of the study. In calculating the number and total area of disturbances, we included all disturbed areas that were inside the plot boundaries (if a disturbance was on the boundary, only the area inside the plot was included). Our analyses of temporal variation employed the same definitions for numbers and areas of canopy disturbances within the 50 ha plot. For analyses of the size structure of disturbances, we included the complete areas of disturbances whose centroids were located within the plot (i.e., we excluded disturbances centered outside the plot, and included area outside the plot for disturbances centered inside the plot to avoid artifacts related to reducing disturbance size by trimming at the plot boundaries).

149

150

2.4 Temporal variation in canopy disturbance rates and its relation to climate

151

152

153

154

155

We calculated canopy disturbances rates for each measurement interval as the % of area disturbed per month (i.e., per 30-day period). Specifically, we summed the total area disturbed during the measurement interval, and divided by the total area of the plot and the length of the time interval. We excluded one excessively long interval (237 days – image acquisition gap) from all analyses of temporal variation; the remaining intervals ranged from 14 to 91 days, with a median of 31.5 days (Table S1). We also calculated an incidence canopy disturbance rate as the number of canopy disturbances per hectare per month. We calculated the

mean, minimum, maximum, and the 25th, 50th, and 75th percentiles of interval length, number and area of canopy disturbances, and the respective monthly rates.

We compared canopy disturbance rates between wet and dry seasons and between early wet and late wet seasons. We defined the dry season as January 1 to April 30 (rainfall < 100 mm mo⁻¹, Fig. S3), the early wet season as 1 May to 31 August, and the late wet season as 1 September to 31 December. Intervals that straddled more than one season were classified to the season in which they had more days. We tested for differences in canopy disturbance rates between seasons using two-tailed Student's t-test on the log-transformed canopy disturbance rates for each measurement interval, after first confirming that these rates met assumptions for normality (Shapiro-Wilk test) and homogeneity of variance (Levene test).

We evaluated the relationship of temporal variation in canopy disturbance rates with temporal variation in the frequencies of climate extremes using parametric correlations. We calculated the Pearson correlations of the log-transformed canopy disturbance rates (area per time) with the log-transformed frequency of extreme rainfall and windspeed events (number per time) (i.e. log(y)~log(x+1)), for different definitions of extreme events. For example, one definition of an extreme event would be a 15-minute period with rainfall above the 99th percentile. We evaluated three different temporal grains for defining extreme events (15-minute, 1-hour, and 1-day intervals), for two different meteorological variables (total rainfall and maximum windspeed), and 100 different thresholds, corresponding to every 0.1 percentile increment between the 90th and 99.9th percentile of the corresponding distributions. We compared the predictive ability of these 600 different definitions of extreme events in terms of their Pearson correlations.

2.5 Size structure of canopy disturbances

We characterized the size structure of canopy disturbances whose geometric center was inside the plot, excluding disturbances from the one excessively long interval of 237 days. Longer time intervals increase the likelihood that what is measured as a single disturbance event in fact constitutes multiple adjoining or overlapping events. We calculated the mean, minimum, maximum, and median of area of individual canopy disturbances. We calculated the cumulative distribution functions with respect to disturbance size (area) of number and total area of canopy disturbances, to quantify the proportions of canopy disturbances and of total area disturbed in disturbances below any given size.

We took advantage of the three-dimensional structure of our photogrammetry data to quantify canopy disturbances in terms of their vertical height drop as well as their horizontal area. For each canopy disturbance, we calculated the average height drop from the differences in the canopy surface models. We excluded 61 canopy disturbances in which mean heights increased because they reflect errors in the canopy height models. We fit a generalized additive model (GAM) for average height drop as a function of the log-transformed area to better visualize the trend in how these were related.

We quantified the size distributions of canopy disturbances by fitting three alternative probability distributions: exponential, power (or Pareto), and Weibull Eqs. (1-3).

$$f_{exp}(x) = \frac{1}{N} \lambda e^{-\lambda x} \quad (1)$$

$$f_{pow}(x) = \frac{1}{N} x^{-\lambda} \quad (2)$$

$$f_{weib}(x) = \frac{1}{N\alpha} \left(\frac{x}{\alpha}\right)^{\lambda-1} e^{-\left(\frac{x}{\alpha}\right)^{\lambda}} \quad (3)$$

188

189 where λ and α are fitted parameters, x is canopy disturbance area in m^2 , e is the natural exponential basis, and N are normalization
 190 constants such that the truncated distribution integrates to 1. Recognizing that our methods are likely to miss smaller disturbances,
 191 we fit these distributions to truncated datasets, excluding disturbances below 2, 5, 10 or 25 m^2 . Note that 25 m^2 is the minimum
 192 area for defining a canopy disturbance in our automated pre-delineation algorithm, and we are confident we captured all
 193 disturbances above this area. We are progressively less confident of our ability to capture smaller disturbances. We also truncated
 194 the fitted distributions above at the maximum possible disturbance area we could have observed using our methods (50 ha, or
 195 500,000 m^2). We fit each type of distribution (exponential, power, Weibull) to each dataset (different minimum disturbance area
 196 and corresponding truncation) using maximum likelihood. The maximum likelihood estimates of the parameters were those that
 197 maximized the likelihood function (Eq. (4)):

$$L = \sum_i \log[f(x)] \quad (4)$$

198 We selected the model that minimized Akaike's Information Criterion (AIC) (Burnham and Anderson, 2002). We also evaluated
 199 goodness of fit using the Kolmogorov-Smirnov statistic, the maximum difference in the cumulative probability distributions
 200 between the observed data and the fitted distribution (Carvalho, 2015).

201 2.6 Branchfalls vs. treefalls

202 We classified each canopy disturbance as being a branchfall, treefall, or standing dead tree, except for those disturbances
 203 occurring in the exceptionally long time interval. In 35 cases we could not distinguish the type of disturbance, and these cases were
 204 omitted from analyses that required disturbance classification. We evaluated the relative contributions of branchfalls vs. treefalls,
 205 and we did not include standing dead trees in the analysis because our methods possibly missed standing dead trees. We separately
 206 calculated treefall and branchfall disturbance rates for each interval, and relative contributions to their summed number and area.
 207 We calculated the Pearson correlations of branchfall disturbance rates with treefall disturbance rates, for both area- and number-
 208 based rates.

209

210 3. Results

211 We identified 1048 canopy disturbances with a combined area of 56,134.37 m^2 (5.61 ha) that affected the area within the
 212 BCI 50 ha plot between 2 October 2014 and 28 November 2019 (Fig. 2). During the 5 years of the study, 11.2 % of the area of the
 213 BCI 50-ha plot was affected by canopy disturbances (Fig. 2), and 0.6 % was disturbed more than once (Fig. S4).

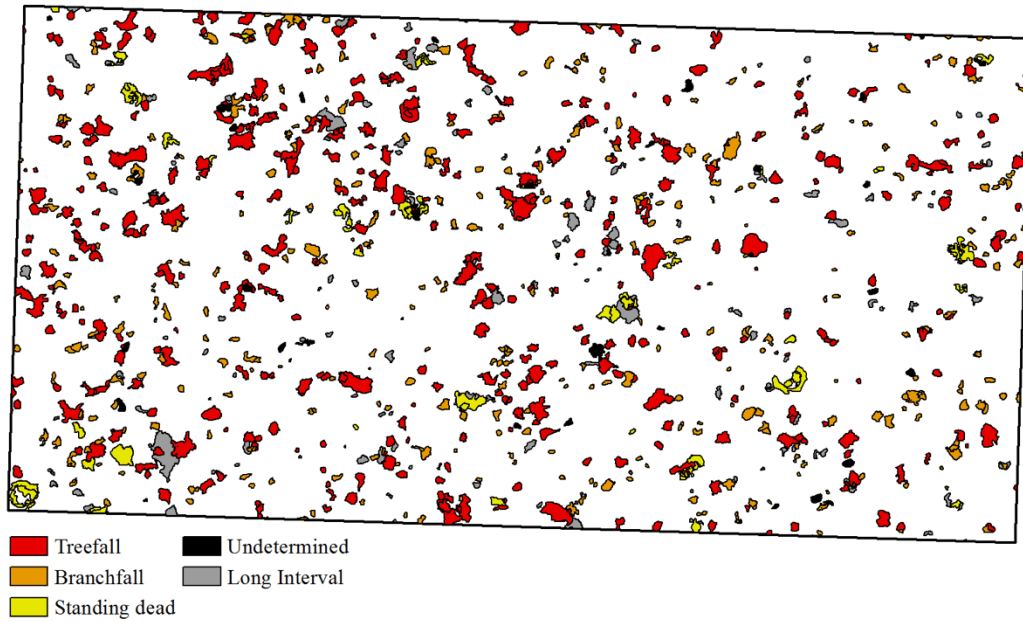


Figure 2. Map of canopy disturbances on the 50 ha plot (black rectangle, 1000 x 500 m) on Barro Colorado Island, Panama, from 2 October 2014 to 28 November 2019.

3.1 Temporal variation in canopy disturbance rates

Temporal variation analyses included 898 disturbances or partial disturbances encompassing 49,742.1 m² of area inside the 50 ha plot in 46 time intervals (excluding the single long interval). There was strong temporal variation in canopy disturbance rates, with similar temporal variation in the total area disturbed (Fig. 3) and in the number of disturbances (Fig. S5). The mean rate of canopy disturbance creation was 905.1 m² mo⁻¹ (range of 75 m² mo⁻¹ to 8040.9 m² mo⁻¹) and the median 499 m² mo⁻¹ (other statistics in Table S1).

The highest disturbance rates occurred during May-July 2016, May-August 2018, and August-September 2019 (Fig. S6). The single highest disturbance rate was observed between 1 June and 13 July 2016, when 11,257 m² of disturbances were created in just 42 days (a rate of 268 m² day⁻¹). A full 2.3 % of the total area of the plot was converted to new canopy disturbances during this time interval.

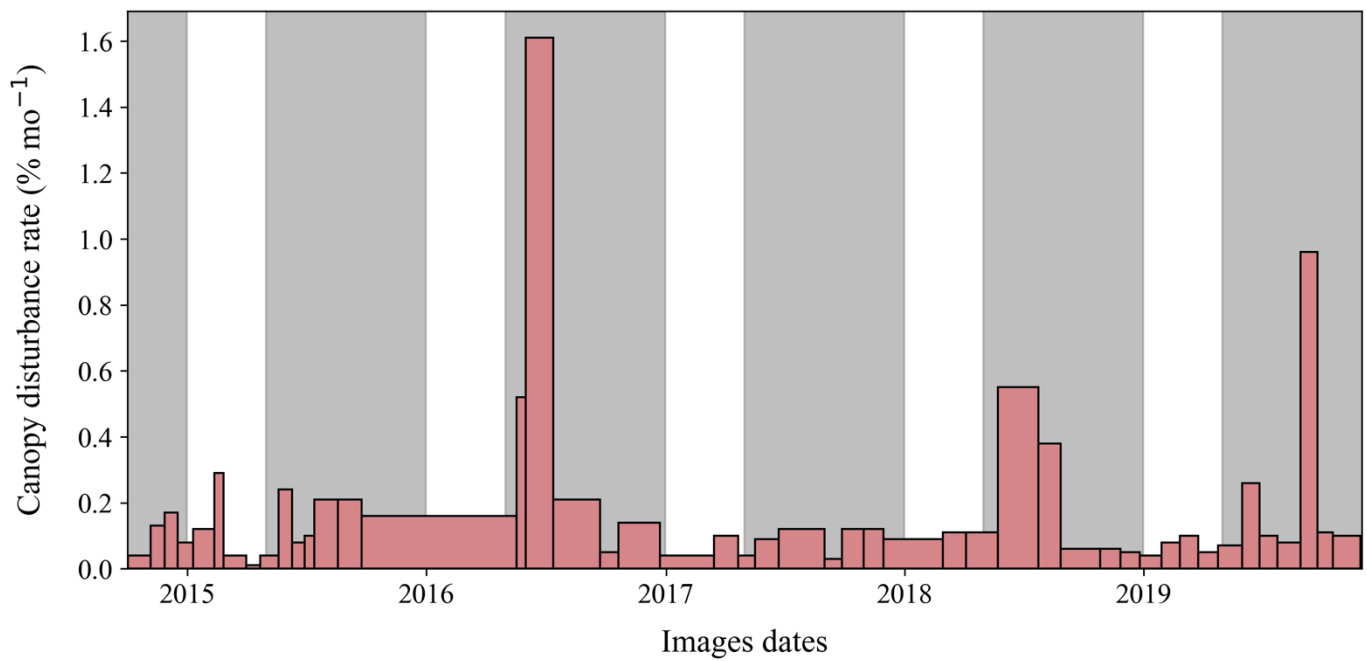


Figure 3. Temporal variation in canopy disturbance rates in the 50 ha plot on Barro Colorado Island, Panama, across measurement intervals. Gray shading indicates the wet seasons (May to December) of each year and ticks on the x axis indicate the first day of each year. Rates are shown in units of percent of area per month (sum of total area disturbed during the measurement interval, divided by the total area of the plot and the length of the time interval times 30-days). Note that the total area of each rectangle is proportional to the total area of canopy disturbed during that measurement interval.

Rates of canopy disturbances were higher during the wet season ($p = 0.036$; Fig. 4a). There was no significant difference in rates between the early and late wet season ($p = 0.226$, Fig. 4b). Very high rates of disturbance (> 0.3 % per month) were observed only in the wet season.

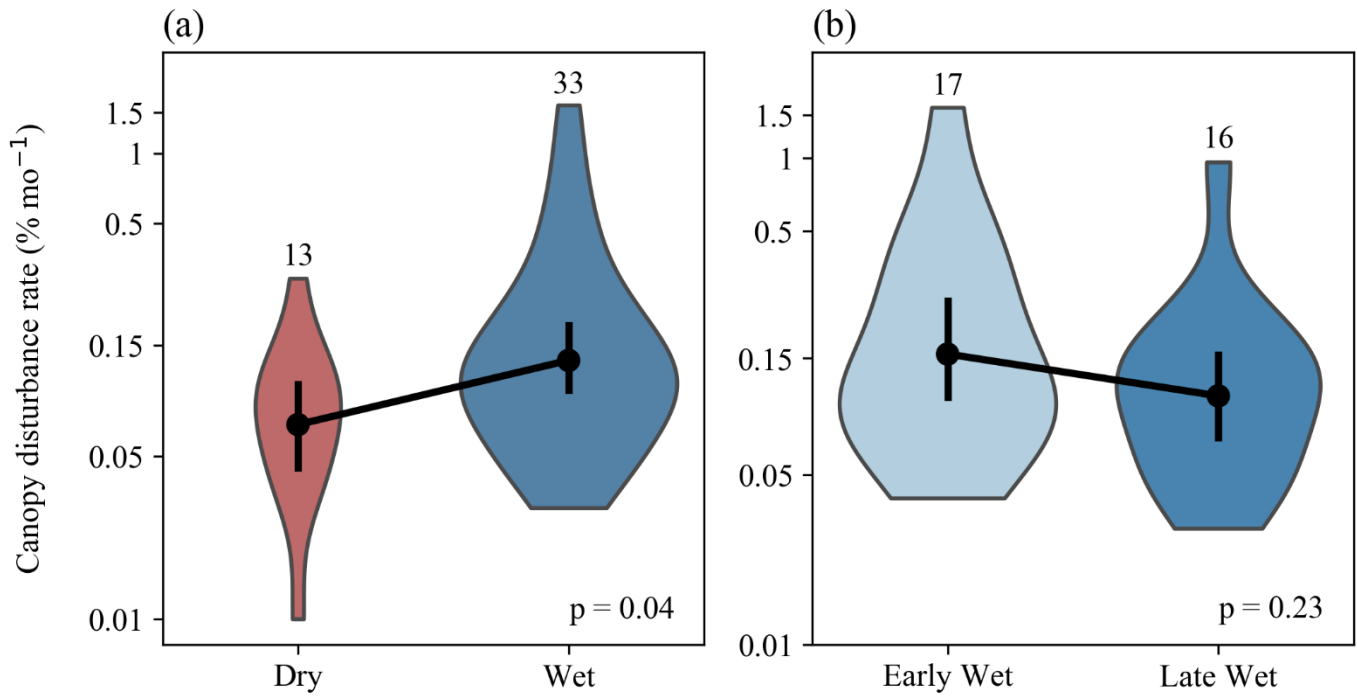


Figure 4. Comparisons of canopy disturbances rates between wet and dry seasons (a), between early and late wet seasons (b). Violin plots depict the distributions of disturbance rates (% area disturbed per month) over time intervals, with the number of time intervals listed above each violin plot. Black dots and bars show mean and 95% confidence intervals, respectively. P-values are based on two-tailed Student's t tests for differences in log-transformed canopy disturbance rates between seasons.

The best correlate of temporal variation in canopy disturbance rates was the frequency of 15-min rainfall events above the 98.2th percentile, which explained 22 % of the variation (Fig. 5a). This relationship was mainly driven by events occurred during wet seasons (Fig. 5a). This threshold outperformed all other tested rainfall thresholds (all percentiles from 90.0 to 99.9, by 0.1 % of the different frequency time scales – Fig. 5b). The 98.2th percentile corresponds to a rainfall rate of 24.3 mm hour⁻¹ (Fig. 5c). There were a total of 141 15-min rainfall events exceeding this threshold, which occurred on 98 different days (Table S2). The measurement interval with the highest disturbance rate (June 1 to July 13 2016) included eleven such high 15-min rainfall events on six days (Table S2). The frequency of high maximum wind speed events was not significantly related with canopy disturbance rates. Indeed, Pearson correlations were negative for most wind speed variables (Fig. S7).

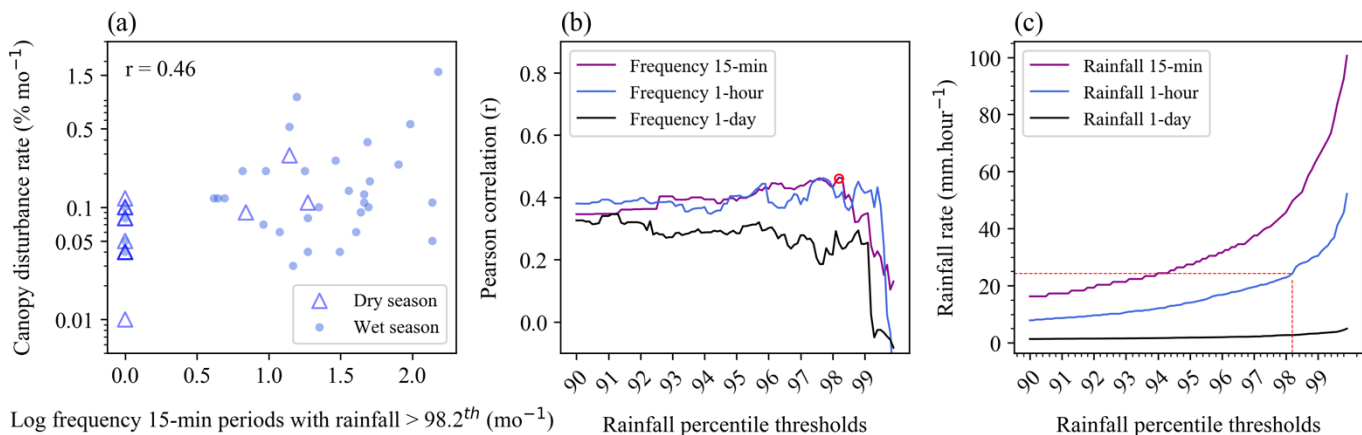


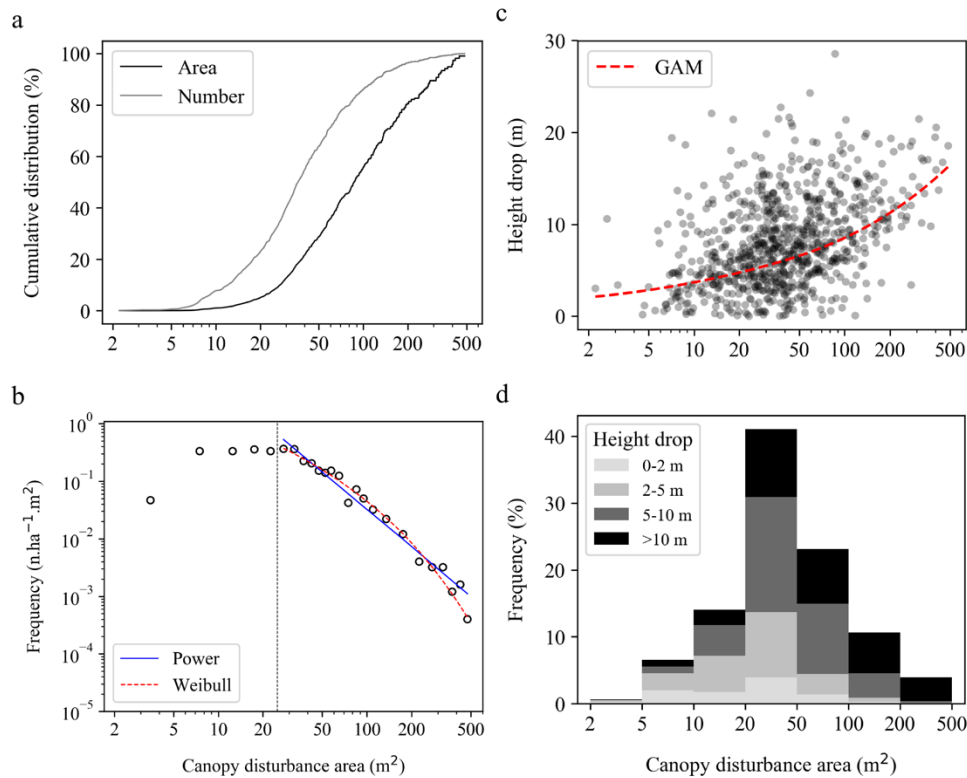
Figure 5. Relation of temporal variation in canopy disturbance rates to the frequency of extreme rainfall events. (a) The relationship for the single best predictor of canopy disturbance rate: the frequency of 15-min periods with rainfall exceeding the 98.2th percentile; each point represents one measurement interval. (b) Variation in Pearson correlation between canopy disturbance rate and frequency of extreme rainfall events depending on the temporal grain (colors) and percentile threshold (x axis) for defining extreme rainfall events, open red circle represents the best correlation. (c) The relationship of percentile threshold (x axis) and rainfall rate (y axis) for different temporal scales. Dashed red line indicates the rainfall rate in mm.hour⁻¹ of the 98.2th percentile.

257

258 3.2 Size structure of canopy disturbances

259 Size distribution analyses included 870 canopy disturbances (with 49,495.5 m² total area) that had their centers inside the
 260 plot and were not part of the excluded long interval. The area of an individual canopy disturbance ranged from 2.2 m² to 486.7 m²,
 261 with a mean of 56.9 m². The median disturbance area was 36.1 m², whereas 50 % of the total area was in disturbances greater than
 262 87.1 m² (Fig. 6a).

263 The size distribution of observed canopy disturbances was close to a power function for areas above 25 m², and was
 264 relatively flat over the range of 5 to 25 m² (Fig. 6b). The fitted exponent of the power function was -2.16 for canopy disturbances
 265 above 25 m², but the Weibull distribution provided a better fit than the power function (Table 1). When distributions were fit to
 266 data including smaller size classes (> 2 m², > 5 m² or > 10 m²), the distribution is further from a power function; the Weibull
 267 remains the best fit, the exponential becomes the second-best fit, and the power function the worst fit of the three (Fig. S8, Fig. S9,
 268 Table 1). Canopy disturbances with larger areas tended to have larger mean decreases in canopy height (Fig. 6c, Fig. 6d).



269

Figure 6. Size structure of canopy disturbances. (a) Cumulative number and area of canopy disturbances in relation to their area. (b) Size distribution of canopy disturbances, together with Weibull and power function fits for canopy disturbances larger than 25 m² (this threshold was chosen because we are confident we identified all canopy disturbances above this area, but we may have missed some smaller ones). (c) Relationship of mean vertical height drop to horizontal area among canopy disturbances. (d) Distribution of canopy disturbances across area and height drop classes. The vertical dashed gray line in b indicates the 25 m² threshold.

Table 1. Parameter values, Kolmogorov-Smirnov statistic, log-likelihood, and delta AIC values for maximum likelihood fits of exponential, power and Weibull probability density functions to size distributions for canopy disturbances larger than 2 m², 5 m², 10 m² and 25 m². Delta AIC is the difference in AIC from the best model. The best-fit models for each dataset, and those within 2 delta AIC of the best model, are highlighted in bold.

| Minimum size (m ²) | Distribution | λ (95% CI) | α (95% CI) | K-S | Log likelihood | Δ AIC |
|--------------------------------|--------------------|---------------------------------|---------------------------|--------------|-----------------|--------------|
| 2 | Exponential | 0.0182 (0.0166 - 0.0199) | | 0.068 | -4354.66 | 0.00 |
| 2 | Power | 1.313 (1.293 - 1.329) | | 0.339 | -4950.99 | 1192.67 |
| 2 | Weibull | 1.027 (0.938 - 1.197) | 55.8 (49.8 - 63.5) | 0.071 | -4354.24 | 1.16 |
| 5 | Exponential | 0.0191 (0.0173 - 0.0211) | | 0.069 | -4286.15 | 4.27 |
| 5 | Power | 1.481 (1.447 - 1.507) | | 0.270 | -4628.98 | 689.94 |
| 5 | Weibull | 0.917 (0.809 - 1.106) | 48.6 (41.3 - 59.3) | 0.055 | -4283.01 | 0.00 |
| 10 | Exponential | 0.0196 (0.0181 - 0.0219) | | 0.076 | -3956.39 | 18.05 |
| 10 | Power | 1.679 (1.644 - 1.711) | | 0.220 | -4131.05 | 367.38 |
| 10 | Weibull | 0.821 (0.732 - 0.978) | 41.0 (33.8 - 50.4) | 0.053 | -3946.36 | 0.00 |
| 25 | Exponential | 0.0197 (0.0180 - 0.0229) | | 0.103 | -2954.95 | 56.59 |
| 25 | Power | 2.162 (2.112 - 2.262) | | 0.080 | -2956.97 | 60.65 |
| 25 | Weibull | 0.529 (0.437 - 0.694) | 12.1 (5.5 - 24.8) | 0.020 | -2925.65 | 0.00 |

3.3 Treefalls and branchfalls

Analyses of the relative contributions of branchfalls, treefalls and standing dead trees included 863 canopy disturbances or partial disturbances with 48,424.7 m² total area inside the 50 ha plot that could be visually classified into one of these categories and that were not part of the excluded long interval. Treefalls accounted for 66.3% of the total observed disturbance area and 47.9% of the total number of observed disturbances; branchfalls accounted for 23.5% of area and 43.5% of number, and standing dead trees accounted for 10.2% of area and 8.6% of number. Treefall and branchfall disturbance rates varied largely in parallel, although the ratios of their rates varied among measurement periods (Fig. 7, Fig. S10). The ratio of area in branchfalls to area in treefalls ranged from 0.024 to 1.4 among measurement periods, and the ratio of number of branchfalls to number of treefalls ranged from 0.083 to 2.3.

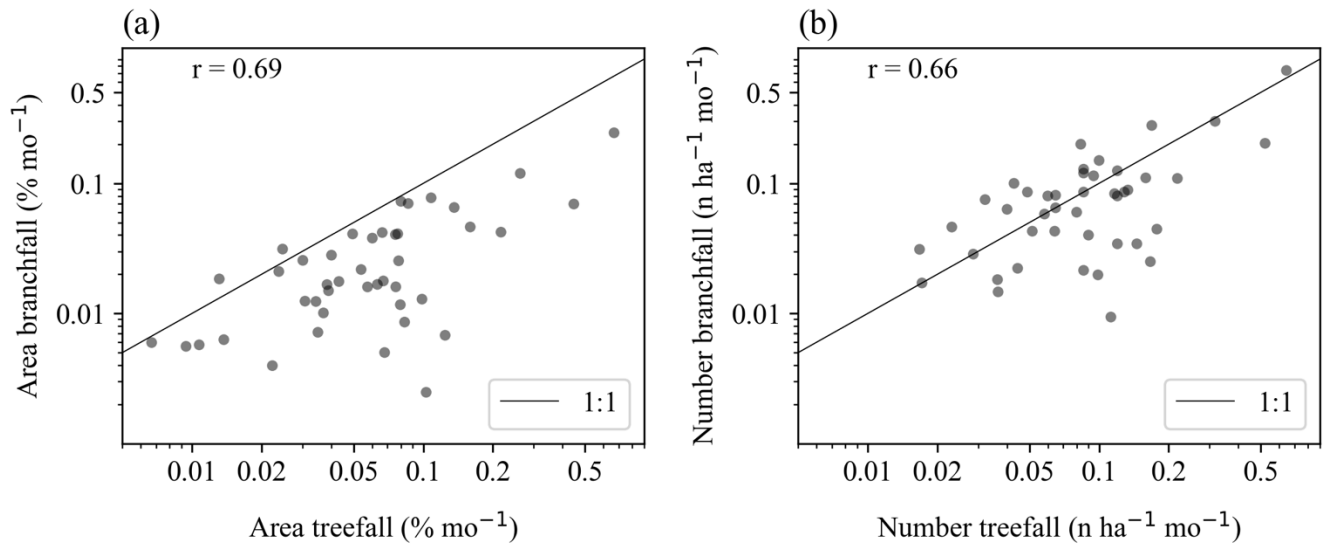


Figure 7. Relationship of temporal variation in branchfall rates to temporal variation in treefall rates, when measured by total area (a) and number of events (b). The 1:1 line is shown for reference.

4. Discussion

The use of high frequency drone imagery enabled us to quantify temporal variation in canopy disturbance rates and to quantify the sizes of canopy disturbances at high temporal and spatial resolutions. We found that canopy disturbance rates of the BCI 50 ha plot varied strongly over time, and were higher in the wet season. The frequency of extreme rainfall events was the best correlate of monthly variation in canopy disturbance rate during the 5-year study period. In contrast, maximum wind speed was not significantly correlated. The size distribution of canopy disturbances was close to a power function for larger canopy disturbances, but best fit by a Weibull function overall. Branchfalls accounted for 26 % of the total area of disturbances from treefalls and branchfalls combined, and branchfall rates varied largely in parallel with treefall rates over time. These findings contributed to improve the understanding of the size distribution, temporal variation and meteorological drivers of canopy disturbances in tropical forests.

4.1 Temporal variation in canopy disturbance

Canopy disturbance rates varied strongly over time in this moist tropical forest, and were higher in the wet season. A single time interval (June 1 to July 13 2016) accounted for 20 % of the total disturbed area of the BCI 50-ha plot. The frequency of extreme rainfall events was a strong correlate of the variation in canopy disturbance rates among measurement intervals, whereas the frequency of high maximum wind speeds was not related. At our site, wind speeds are higher during the dry season, when canopy disturbance rates are lower (Fig. 4a, Fig. S1), and it is possible that wind speed is systematically underestimated in periods of high rainfall. We also note that wind speed and rainfall measurements were from a site 1.7 km from the boundary of the plot. Given the highly local nature of convective storms in the tropics, these measurements are imperfect proxies for conditions in the focal plot. Treefall and branchfall disturbance rates varied largely in parallel, but not entirely. Differences in temporal patterns could in part reflect different sensitivity to particular abiotic drivers (e.g. wind regime, soil saturation).

These results are consistent with previous findings on seasonal variation and the role of rainfall in gap formation in tropical forests. A previous 4-year study on BCI found seasonal peaks in August and September, in the middle of the wet season, with monthly treefall rates significantly correlated with rainfall ($r = 0.47$, $p < 0.02$) (Brokaw, 1982). Monthly tree mortality was also strongly and positively correlated with rainfall ($r = 0.85$) in a 1-year study of a 10-ha site in the Central Amazon (Fontes et al., 2018). Similarly, a study monitoring canopy trees monthly over five decades in the Central Amazon found that trees died more often during wet months, even in drought years (Aleixo et al., 2019). A regional study of the Central Amazon based on 12 years of satellite data found that major windthrows (visible on LANDSAT) occurred more frequently between September and February, months characterized by heavy rainfall, than the rest of the year (Negrón-Juárez et al., 2017). Studies have highlighted the importance of mesoscale convective systems, such as squall lines, for windthrows (Garstang et al., 1998; Negrón-Juárez et al., 2010, 2017; Araujo et al., 2017). In Panama, the period of June to August has the higher number of mesoscale convective systems (Jaramillo et al., 2017), and these were the months when we observed the highest canopy disturbance rates. The threshold rainfall rate of $24.3 \text{ mm hour}^{-1}$, which defined the extreme rainfall rate that was the best predictor of canopy disturbance formation in our study, is four times higher than the mean rate for mesoscale convective systems in the Panama region (Jaramillo et al., 2017), highlighting the importance of extreme events. Analysis of spatial variation in forest damage from Hurricane María in Puerto Rico found that total rainfall was the most important meteorological risk factor and maximum sustained one-minute wind speeds the second-most-important; these two variables were moderately correlated ($r = 0.43$) (Hall et al., 2020).

4.2 Mechanisms and size structure canopy disturbances

Gaps in the forest canopy can be caused proximally by treefalls of canopy trees, branchfalls of canopy branches, the decay of standing dead canopy trees, or the decay of canopy branches. Treefalls and branchfalls of canopy trees are well-captured in our analyses, which focus on short-term changes that indicate loss of major canopy elements. In contrast, the decay of dead trees and senescing branches generally involves more subtle changes in the canopy over a longer period of time, and is possibly mostly missed by our methods. Treefalls account for a majority of canopy tree mortality in most tropical forests, but standing tree mortality also plays a major role, especially in drought periods. Overall, treefalls (in which trees were uprooted or their trunks snapped) accounted for 51.2 % of all mortality of trees $> 10 \text{ cm DBH}$ in a large-scale study of tree mortality in 189 Amazonian plots (Esquivel-Muelbert et al., 2020) and 65 % in a study that monitored tree mortality in 10 ha of forest in the Central Amazon bi-monthly over one year (Fontes et al., 2018). Treefalls can involve a single canopy tree, or multiple canopy trees. Multi-tree treefalls can result from coordinated disturbances over a large area (e.g., large footprint wind disturbance) and/or from domino effects in which the failure of one canopy tree directly stresses one or more neighboring trees and causes them to fall as well (e.g., when additional trees are knocked down by the first tree, or pulled down because of connections via lianas). It has been hypothesized that canopy disturbances may also be contagious over longer time intervals, with increased risk of treefall near canopy gaps, but evidence for this in tropical forests is mixed (Jansen et al., 2008). Given that our measurement intervals are relatively short (~one month), almost all of our mapped canopy disturbances are likely to reflect single catastrophic events.

Our study is one of several that have documented size distributions of canopy disturbances (dynamic gaps) or of static canopy gaps above some size that are approximately power functions, both on BCI (Solé and Manrubia, 1995; Lobo and Dalling, 2014) and in other tropical forests (Marvin and Asner, 2016; Asner et al., 2013; Kellner and Asner, 2009; Silva et al., 2019; Fisher et al., 2008). Static canopy gaps are areas in which the forest canopy is below a threshold height, e.g., 10 m, at a given time. A

power function distribution of disturbance event sizes (here canopy disturbances) and of the sizes of disturbed areas (canopy gaps) can emerge from self-organization of dynamic systems such as forests in which individual tree growth and death depend on the sizes of neighbors (Solé and Manrubia, 1995). These same self-organized dynamics lead to the development of equilibrium size distributions of trees, which are typically well-fit by Weibull distributions in tropical forests (Muller-Landau et al., 2006b, a). The relative dearth of canopy disturbances smaller than 25 m² in our dataset, compared to what would be expected under a power function, may be explained in part by lower detection frequencies, i.e., measurement bias. Our methods are expected to capture all treefall and branchfalls above this threshold, but we may increasingly have missed smaller events, especially below ~ 5 m². However, we consider it unlikely that this is a sufficient explanation for the shortfall in small disturbances, and suggest that it is more likely explained largely by the low frequency of small trees and branches in the canopy of this mature tropical forest, and thus a dearth of small treefall and branchfall events.

Although rarely quantified, branchfall is an important ecological process, with major contributions to woody turnover and necromass production. We found that branchfalls were almost as common as treefalls in number, although they contributed a substantially smaller total area of disturbance. Similarly, a ground survey of 78 canopy turnover events in a Brazilian Amazon forest found that 44 % were branchfalls, and accounted for 15 % of the total affected area (Leitold et al., 2018). In contrast, a landscape level analysis of LiDAR data concluded that branchfalls were seven times more frequent than treefalls and accounted for five times more area (Marvin and Asner, 2016). However, Marvin and Asner (2016) classified branchfalls and treefalls based purely on the proportional decrease in canopy height (10-40 % decrease and 70-100 % decrease, respectively), a process liable to misclassification. It entirely ignored disturbances involving intermediate decreases in canopy height (40-70 %), and did not consider the possibility that any of these disturbances might be standing dead trees. Thus the differences in branchfall contribution between our work and that of Marvin and Asner (Marvin and Asner, 2016) may be due as much to methodological differences as to real variation in canopy dynamics.

374

375 5. Conclusions and future directions

A mechanistic understanding of the controls on woody residence time in tropical forests is urgently needed to predict the future of tropical forest carbon stocks and biodiversity under global change (Johnson et al., 2016; McDowell et al., 2018; Muller-Landau et al., 2021). Canopy trees account for a majority of the productivity and carbon stocks in tropical forests, and their fates are disproportionately important for determining stand-level woody residence time (Araujo et al., 2020). Advances in drone hardware and photogrammetric software now make it relatively inexpensive and straightforward to quantify forest canopy structure and dynamics at high spatial and temporal resolution through digital aerial photogrammetry and repeat drone imagery acquisitions. Here we applied these methods to 50 ha of old-growth tropical forest for 5 years, and analyzed the resulting products to quantify major drops in canopy height such as those created by branchfalls and treefalls, and thus calculate the canopy disturbance rate. We found that canopy disturbance rates are highly temporally variable, and are well-predicted by extreme rainstorms. Spatial resolutions of 3-7 cm in the orthomosaics, as used here, are now easily attained, and proved sufficient to capture canopy dynamics and visually classify disturbances as treefalls, branchfalls, or decomposition of standing dead trees.

Future research building on these approaches and expanding them to additional sites has much to contribute to our understanding of tropical forest dynamics. The relationship of standing dead tree mortality to temporal climate variation could be investigated from these same data by conducting additional analyses of the orthomosaics to quantify temporal changes in leafing

status of standing dead trees, prior to these trees decomposing. A better understanding of the relationship of storm conditions to treefall and branchfall rates could be obtained by combining such drone-acquired data with mechanistic models of wind damage risk (Jackson et al., 2019), collecting higher frequency three-dimensional wind data, and/or measuring canopy dynamics at even higher temporal resolution. The use of drones with high accuracy GPS systems, either post-processed kinematic (PPK) or real-time kinematic (RTK) systems, would also be advantageous, and could enable elimination of the alignment step of the processing as well as automation of the identification of canopy disturbances based on elevation model differences alone. Finally, we recommend carrying out flights under cloudy conditions when possible, as these diffuse lighting conditions improve visibility deeper in the canopy and reduce complications associated with shadows. The expansion of these methods to additional and larger areas, potentially in part through citizen science initiatives, has great potential to improve our understanding of tropical forest tree mortality, and the future of tropical forests under changing climate regimes.

400

Code and data availability. Analysis codes, input data and output results are available at https://github.com/Raquel-Araujo/gap_dynamics_BCI50ha. All files will be published in a permanent form at Smithsonian Figshare repository 10.25573/data.c.5389043 when the manuscript is published.

404

Author contributions. HCM and RFA planned and designed the research. MG and JD collected drone data. RFA, SG, JD and MG processed drone imagery. RFA performed the analysis with support from HCM, CHSC and RINJ. RFA and HCM wrote the manuscript.

408

Competing interests. The authors declare that they have no conflicts of interest.

410

Acknowledgments. We gratefully acknowledge the financial support of the Next Generation Ecosystem Experiments-Tropics, funded by the U.S. Department of Energy, Office of Science, Office of Biological and Environmental Research (RFA), the Smithsonian Institution Competitive Grants Program for Science (HCM, JD), and the Smithsonian Tropical Research Institute fellowship program (CHSC, RFA). We thank Milton Solano, Pablo Ramos, and Paulino Villareal for assistance in collecting and processing the drone imagery, and Jeffrey Chambers, KC Cushman and Evan Gora for providing helpful comments on an earlier version of this manuscript.

417

418 **References**

Aleixo, I., Norris, D., Hemerik, L., Barbosa, A., Prata, E., Costa, F., and Poorter, L.: Amazonian rainforest tree mortality driven by climate and functional traits, *Nat. Clim. Chang.*, 9, 384–388, <https://doi.org/10.1038/s41558-019-0458-0>, 2019.

422 Araujo, R. F., Nelson, B. W., Celes, C. H. S., and Chambers, J. Q.: Regional distribution of large
 423 blowdown patches across Amazonia in 2005 caused by a single convective squall line: Distribution of
 424 Amazonia Blowdown Damage, *Geophys. Res. Lett.*, 44, 7793–7798,
 425 <https://doi.org/10.1002/2017GL073564>, 2017.

426 Araujo, R. F., Chambers, J. Q., Celes, C. H. S., Muller-Landau, H. C., Santos, A. P. F. dos, Emmert, F.,
 427 Ribeiro, G. H. P. M., Gimenez, B. O., Lima, A. J. N., Campos, M. A. A., and Higuchi, N.: Integrating high
 428 resolution drone imagery and forest inventory to distinguish canopy and understory trees and quantify their
 429 contributions to forest structure and dynamics, *PLoS ONE*, 15, e0243079,
 430 <https://doi.org/10.1371/journal.pone.0243079>, 2020.

431 Arellano, G., Medina, N. G., Tan, S., Mohamad, M., and Davies, S. J.: Crown damage and the mortality of
 432 tropical trees, *New Phytol*, 221, 169–179, <https://doi.org/10.1111/nph.15381>, 2019.

433 Asner, G. P., Kellner, J. R., Kennedy-Bowdoin, T., Knapp, D. E., Anderson, C., and Martin, R. E.: Forest
 434 Canopy Gap Distributions in the Southern Peruvian Amazon, *PLoS ONE*, 8, e60875,
 435 <https://doi.org/10.1371/journal.pone.0060875>, 2013.

436 Aubry-Kientz, M., Rossi, V., Cornu, G., Wagner, F., and Hérault, B.: Temperature rising would slow down
 437 tropical forest dynamic in the Guiana Shield, *Sci Rep*, 9, 10235, [https://doi.org/10.1038/s41598-019-46597-](https://doi.org/10.1038/s41598-019-46597-8)
 438 8, 2019.

439 Brien, R. J. W., Phillips, O. L., Feldpausch, T. R., Gloor, E., Baker, T. R., Lloyd, J., Lopez-Gonzalez, G.,
 440 Monteagudo-Mendoza, A., Malhi, Y., Lewis, S. L., Vásquez Martinez, R., Alexiades, M., Álvarez Dávila,
 441 E., Alvarez-Loayza, P., Andrade, A., Aragão, L. E. O. C., Araujo-Murakami, A., Arets, E. J. M. M.,
 442 Arroyo, L., Aymard C., G. A., Bánki, O. S., Baraloto, C., Barroso, J., Bonal, D., Boot, R. G. A., Camargo,
 443 J. L. C., Castilho, C. V., Chama, V., Chao, K. J., Chave, J., Comiskey, J. A., Cornejo Valverde, F., da
 444 Costa, L., de Oliveira, E. A., Di Fiore, A., Erwin, T. L., Fauset, S., Forsthofer, M., Galbraith, D. R.,
 445 Grahame, E. S., Groot, N., Hérault, B., Higuchi, N., Honorio Coronado, E. N., Keeling, H., Killeen, T. J.,
 446 Laurance, W. F., Laurance, S., Licona, J., Magnussen, W. E., Marimon, B. S., Marimon-Junior, B. H.,
 447 Mendoza, C., Neill, D. A., Nogueira, E. M., Núñez, P., Pallqui Camacho, N. C., Parada, A., Pardo-Molina,
 448 G., Peacock, J., Peña-Claros, M., Pickavance, G. C., Pitman, N. C. A., Poorter, L., Prieto, A., Quesada, C.
 449 A., Ramírez, F., Ramírez-Angulo, H., Restrepo, Z., Roopsind, A., Rudas, A., Salomão, R. P., Schwarz, M.,
 450 Silva, N., Silva-Espejo, J. E., Silveira, M., Stropp, J., Talbot, J., ter Steege, H., Teran-Aguilar, J., Terborgh,
 451 J., Thomas-Caesar, R., Toledo, M., Torello-Raventos, M., Umetsu, R. K., van der Heijden, G. M. F., van
 452 der Hout, P., Guimarães Vieira, I. C., Vieira, S. A., Vilanova, E., Vos, V. A., and Zagt, R. J.: Long-term
 453 decline of the Amazon carbon sink, *Nature*, 519, 344–348, <https://doi.org/10.1038/nature14283>, 2015.

454 Brokaw, N. V. L.: Treefalls: frequency, timing, and consequences., in: *The ecology of a tropical forest:*
 455 *seasonal rhythms and long-term changes*, Smithsonian Institution, Washington, DC, 101–108, 1982.

456 Brokaw, N. V. L.: Gap-Phase Regeneration in a Tropical Forest, 66, 682–687,
 457 <https://doi.org/10.2307/1940529>, 1985.

458 Burnham, K. P. and Anderson, D. R.: Model selection and multimodel inference: a practical information-
 459 theoretic approach, 2nd ed., Springer-Verlag New York, New York, 2002.

460 Carvalho, L.: An Improved Evaluation of Kolmogorov’s Distribution, *J. Stat. Soft.*, 65,
 461 <https://doi.org/10.18637/jss.v065.c03>, 2015.

462 Cavaleri, M. A., Reed, S. C., Smith, W. K., and Wood, T. E.: Urgent need for warming experiments in
463 tropical forests, *Glob Change Biol*, 21, 2111–2121, <https://doi.org/10.1111/gcb.12860>, 2015.

464 Dalagnol, R., Wagner, F. H., Galvão, L. S., Streher, A. S., Phillips, O. L., Gloor, E., Pugh, T. A. M.,
465 Ometto, J. P. H. B., and Aragão, L. E. O. C.: Large-scale variations in the dynamics of Amazon forest
466 canopy gaps from airborne lidar data and opportunities for tree mortality estimates, *Sci Rep*, 11, 1388,
467 <https://doi.org/10.1038/s41598-020-80809-w>, 2021.

468 Dalling, J. W., Winter, K., and Hubbell, S. P.: Variation in growth responses of neotropical pioneers to
469 simulated forest gaps, *Funct Ecology*, 18, 725–736, <https://doi.org/10.1111/j.0269-8463.2004.00868.x>,
470 2004.

471 Dandois, J. P. and Ellis, E. C.: High spatial resolution three-dimensional mapping of vegetation spectral
472 dynamics using computer vision, *Remote Sensing of Environment*, 136, 259–276,
473 <https://doi.org/10.1016/j.rse.2013.04.005>, 2013.

474 Davies, S. J., Abiem, I., Abu Salim, K., Aguilar, S., Allen, D., Alonso, A., Anderson-Teixeira, K., Andrade,
475 A., Arellano, G., Ashton, P. S., Baker, P. J., Baker, M. E., Baltzer, J. L., Basset, Y., Bissengou, P.,
476 Bohlman, S., Bourg, N. A., Brockelman, W. Y., Bunyavejchewin, S., Burslem, D. F. R. P., Cao, M.,
477 Cárdenas, D., Chang, L.-W., Chang-Yang, C.-H., Chao, K.-J., Chao, W.-C., Chapman, H., Chen, Y.-Y.,
478 Chisholm, R. A., Chu, C., Chuyong, G., Clay, K., Comita, L. S., Condit, R., Cordell, S., Dattaraja, H. S., de
479 Oliveira, A. A., den Ouden, J., Detto, M., Dick, C., Du, X., Duque, Á., Ediriweera, S., Ellis, E. C., Obiang,
480 N. L. E., Esufali, S., Ewango, C. E. N., Fernando, E. S., Filip, J., Fischer, G. A., Foster, R., Giambelluca,
481 T., Giardina, C., Gilbert, G. S., Gonzalez-Akre, E., Gunatilleke, I. A. U. N., Gunatilleke, C. V. S., Hao, Z.,
482 Hau, B. C. H., He, F., Ni, H., Howe, R. W., Hubbell, S. P., Huth, A., Inman-Narahari, F., Itoh, A., Janík,
483 D., Jansen, P. A., Jiang, M., Johnson, D. J., Jones, F. A., Kanzaki, M., Kenfack, D., Kiratiprayoon, S., Král,
484 K., Krizel, L., Lao, S., Larson, A. J., Li, Y., Li, X., Litton, C. M., Liu, Y., Liu, S., Lum, S. K. Y., Luskin,
485 M. S., Lutz, J. A., Luu, H. T., Ma, K., Makana, J.-R., Malhi, Y., Martin, A., McCarthy, C., McMahon, S.
486 M., McShea, W. J., Memiaghe, H., Mi, X., Mitre, D., Mohamad, M., Monks, L., et al.: ForestGEO:
487 Understanding forest diversity and dynamics through a global observatory network, *Biological*
488 *Conservation*, 253, 108907, <https://doi.org/10.1016/j.biocon.2020.108907>, 2021.

489 Deb, J., Phinn, S., Butt, N., and Mcalpine, C.: Climate change impacts on tropical forests: identifying risks
490 for tropical Asia, *JTFS*, 30, 182–194, <https://doi.org/10.26525/jtfs2018.30.2.182194>, 2018.

491 Denslow, J. S.: Patterns of plant species diversity during succession under different disturbance regimes,
492 *Oecologia*, 46, 18–21, <https://doi.org/10.1007/BF00346960>, 1980.

493 Denslow, J. S.: Tropical Rainforest Gaps and Tree Species Diversity, 1, 431–451, 1987.

494 Esquivel-Muelbert, A., Phillips, O. L., Brien, R. J. W., Fauset, S., Sullivan, M. J. P., Baker, T. R., Chao,
495 K.-J., Feldpausch, T. R., Gloor, E., Higuchi, N., Houwing-Duistermaat, J., Lloyd, J., Liu, H., Malhi, Y.,
496 Marimon, B., Marimon Junior, B. H., Monteagudo-Mendoza, A., Poorter, L., Silveira, M., Torre, E. V.,
497 Dávila, E. A., del Aguila Pasquel, J., Almeida, E., Loayza, P. A., Andrade, A., Aragão, L. E. O. C., Araujo-
498 Murakami, A., Arets, E., Arroyo, L., Aymard, C., G. A., Baisie, M., Baraloto, C., Camargo, P. B., Barroso,
499 J., Blanc, L., Bonal, D., Bongers, F., Boot, R., Brown, F., Burban, B., Camargo, J. L., Castro, W., Moscoso,
500 V. C., Chave, J., Comiskey, J., Valverde, F. C., da Costa, A. L., Cardozo, N. D., Di Fiore, A., Dourdain, A.,
501 Erwin, T., Llampazo, G. F., Vieira, I. C. G., Herrera, R., Honorio Coronado, E., Huamantupa-Chuquimaco,
502 I., Jimenez-Rojas, E., Killeen, T., Laurance, S., Laurance, W., Levesley, A., Lewis, S. L., Ladvocat, K. L.
503 L. M., Lopez-Gonzalez, G., Lovejoy, T., Meir, P., Mendoza, C., Morandi, P., Neill, D., Nogueira Lima, A.
504 J., Vargas, P. N., de Oliveira, E. A., Camacho, N. P., Pardo, G., Peacock, J., Peña-Claros, M., Peñuela-

505 Mora, M. C., Pickavance, G., Pipoly, J., Pitman, N., Prieto, A., Pugh, T. A. M., Quesada, C., Ramirez-
506 Angulo, H., de Almeida Reis, S. M., Rejou-Machain, M., Correa, Z. R., Bayona, L. R., Rudas, A.,
507 Salomão, R., Serrano, J., Espejo, J. S., Silva, N., Singh, J., Stahl, C., Stropp, J., Swamy, V., Talbot, J., ter
508 Steege, H., et al.: Tree mode of death and mortality risk factors across Amazon forests, *Nat Commun*, 11,
509 5515, <https://doi.org/10.1038/s41467-020-18996-3>, 2020.

510 Fisher, J. I., Hurtt, G. C., Thomas, R. Q., and Chambers, J. Q.: Clustered disturbances lead to bias in large-
511 scale estimates based on forest sample plots: Clustered disturbance and forest plot bias, 11, 554–563,
512 <https://doi.org/10.1111/j.1461-0248.2008.01169.x>, 2008.

513 Fontes, C. G., Chambers, J. Q., and Higuchi, N.: Revealing the causes and temporal distribution of tree
514 mortality in Central Amazonia, *Forest Ecology and Management*, 424, 177–183,
515 <https://doi.org/10.1016/j.foreco.2018.05.002>, 2018.

516 Garstang, M., White, S., Shugart, H. H., and Halverson, J.: Convective cloud downdrafts as the cause of
517 large blowdowns in the Amazon rainforest, *Meteorol. Atmos. Phys.*, 67, 199–212,
518 <https://doi.org/10.1007/BF01277510>, 1998.

519 Hall, J., Muscarella, R., Quebbeman, A., Arellano, G., Thompson, J., Zimmerman, J. K., and Uriarte, M.:
520 Hurricane-Induced Rainfall is a Stronger Predictor of Tropical Forest Damage in Puerto Rico Than
521 Maximum Wind Speeds, *Sci Rep*, 10, 4318, <https://doi.org/10.1038/s41598-020-61164-2>, 2020.

522 Harms, K. E., Condit, R., Hubbell, S. P., and Foster, R. B.: Habitat associations of trees and shrubs in a 50-
523 ha neotropical forest plot: *Habitat associations of trees and shrubs*, 89, 947–959,
524 <https://doi.org/10.1111/j.1365-2745.2001.00615.x>, 2001.

525 Holdridge, L. R.: Determination of World Plant Formations from Simple Climatic Data, 105, 367–368,
526 1947.

527 Hubbell, S. P., Foster, R. B., O’Brien, S. T., Harms, K. E., Condit, R., Wechsler, B., Wright, S. J., and Loo
528 de Lao, S.: Light-Gap Disturbances, Recruitment Limitation, and Tree Diversity in a Neotropical Forest,
529 283, 554–557, <https://doi.org/10.1126/science.283.5401.554>, 1999.

530 IPCC: Summary for Policymakers, in: *Climate Change 2014, Mitigation of Climate Change. Contribution*
531 *of Working Group III to the Fifth Assessment Report of the Intergovernmental Panel on Climate Change*,
532 Cambridge University Press, United Kingdom and New York, NY, USA, 2014.

533 Jackson, T., Shenkin, A., Wellpott, A., Calders, K., Origo, N., Disney, M., Burt, A., Raunonen, P.,
534 Gardiner, B., Herold, M., Fourcaud, T., and Malhi, Y.: Finite element analysis of trees in the wind based on
535 terrestrial laser scanning data, *Agricultural and Forest Meteorology*, 265, 137–144,
536 <https://doi.org/10.1016/j.agrformet.2018.11.014>, 2019.

537 Jansen, P. A., Meer, P. J. V. der, and Bongers, F.: Spatial contagiousness of canopy disturbance in tropical
538 rain forest: An individual-tree-based test, *Ecology*, 89, 3490–3502, <https://doi.org/10.1890/07-1682.1>,
539 2008.

540 Jaramillo, L., Poveda, G., and Mejía, J. F.: Mesoscale convective systems and other precipitation features
541 over the tropical Americas and surrounding seas as seen by TRMM, *Int. J. Climatol*, 37, 380–397,
542 <https://doi.org/10.1002/joc.5009>, 2017.

543 Johnson, M. O., Galbraith, D., Gloor, M., De Deurwaerder, H., Guimberteau, M., Rammig, A., Thonicke,
544 K., Verbeeck, H., Randow, C., Monteagudo, A., Phillips, O. L., Brien, R. J. W., Feldpausch, T. R., Lopez

545 Gonzalez, G., Fauset, S., Quesada, C. A., Christoffersen, B., Ciais, P., Sampaio, G., Kruijt, B., Meir, P.,
546 Moorcroft, P., Zhang, K., Alvarez-Davila, E., Alves de Oliveira, A., Amaral, I., Andrade, A., Aragao, L. E.
547 O. C., Araujo-Murakami, A., Arets, E. J. M. M., Arroyo, L., Aymard, G. A., Baraloto, C., Barroso, J.,
548 Bonal, D., Boot, R., Camargo, J., Chave, J., Cogollo, A., Cornejo Valverde, F., Lola da Costa, A. C., Di
549 Fiore, A., Ferreira, L., Higuchi, N., Honorio, E. N., Killeen, T. J., Laurance, S. G., Laurance, W. F., Licona,
550 J., Lovejoy, T., Malhi, Y., Marimon, B., Marimon, B. H., Matos, D. C. L., Mendoza, C., Neill, D. A.,
551 Pardo, G., Peña-Claros, M., Pitman, N. C. A., Poorter, L., Prieto, A., Ramirez-Angulo, H., Roopsind, A.,
552 Rudas, A., Salomao, R. P., Silveira, M., Stropp, J., Steege, H., Terborgh, J., Thomas, R., Toledo, M.,
553 Torres-Lezama, A., Heijden, G. M. F., Vasquez, R., Guimarães Vieira, I. C., Vilanova, E., Vos, V. A., and
554 Baker, T. R.: Variation in stem mortality rates determines patterns of above-ground biomass in Amazonian
555 forests: implications for dynamic global vegetation models, *Glob Change Biol*, 22, 3996–4013,
556 <https://doi.org/10.1111/gcb.13315>, 2016.

557 Kellner, J. R. and Asner, G. P.: Convergent structural responses of tropical forests to diverse disturbance
558 regimes, 12, 887–897, <https://doi.org/10.1111/j.1461-0248.2009.01345.x>, 2009.

559 Leigh, E. G. Jr.: Tropical forest ecology: a view from Barro Colorado Island, Oxford University Press,
560 Oxford, 1999.

561 Leitold, V., Morton, D. C., Longo, M., dos-Santos, M. N., Keller, M., and Scaranello, M.: El Niño drought
562 increased canopy turnover in Amazon forests, *New Phytol*, 219, 959–971,
563 <https://doi.org/10.1111/nph.15110>, 2018.

564 Lobo, E. and Dalling, J. W.: Effects of topography, soil type and forest age on the frequency and size
565 distribution of canopy gap disturbances in a tropical forest, *Biogeosciences*, 10, 6769–6781,
566 <https://doi.org/10.5194/bg-10-6769-2013>, 2013.

567 Lobo, E. and Dalling, J. W.: Spatial scale and sampling resolution affect measures of gap disturbance in a
568 lowland tropical forest: implications for understanding forest regeneration and carbon storage, *Proc. R. Soc.*
569 *B.*, 281, 20133218, <https://doi.org/10.1098/rspb.2013.3218>, 2014.

570 Manrubia, S. C. and Solé, R. V.: On Forest Spatial Dynamics with Gap Formation, *Journal of Theoretical*
571 *Biology*, 187, 159–164, <https://doi.org/10.1006/jtbi.1997.0409>, 1997.

572 Marra, D. M., Chambers, J. Q., Higuchi, N., and Trumbore, S. E.: Large-Scale Wind Disturbances Promote
573 Tree Diversity in a Central Amazon Forest, 9, 16, 2014.

574 Marvin, D. C. and Asner, G. P.: Branchfall dominates annual carbon flux across lowland Amazonian
575 forests, *Environ. Res. Lett.*, 11, 094027, <https://doi.org/10.1088/1748-9326/11/9/094027>, 2016.

576 McDowell, N., Allen, C. D., Anderson-Teixeira, K., Brando, P., Brien, R., Chambers, J., Christoffersen,
577 B., Davies, S., Doughty, C., Duque, A., Espirito-Santo, F., Fisher, R., Fontes, C. G., Galbraith, D.,
578 Goodsman, D., Grossiord, C., Hartmann, H., Holm, J., Johnson, D. J., Kassim, Abd. R., Keller, M., Koven,
579 C., Kueppers, L., Kumagai, T., Malhi, Y., McMahon, S. M., Mencuccini, M., Meir, P., Moorcroft, P.,
580 Muller-Landau, H. C., Phillips, O. L., Powell, T., Sierra, C. A., Sperry, J., Warren, J., Xu, C., and Xu, X.:
581 Drivers and mechanisms of tree mortality in moist tropical forests, *New Phytol*, 219, 851–869,
582 <https://doi.org/10.1111/nph.15027>, 2018.

583 McMahon, S. M., Arellano, G., and Davies, S. J.: The importance and challenges of detecting changes in
584 forest mortality rates, *Ecosphere*, 10, e02615, <https://doi.org/10.1002/ecs2.2615>, 2019.

585 Muller-Landau, H. C., Condit, R. S., Harms, K. E., Marks, C. O., Thomas, S. C., Bunyavejchewin, S.,
586 Chuyong, G., Co, L., Davies, S., Foster, R., Gunatilleke, S., Gunatilleke, N., Hart, T., Hubbell, S. P., Itoh,
587 A., Kassim, A. R., Kenfack, D., LaFrankie, J. V., Lagunzad, D., Lee, H. S., Losos, E., Makana, J.-R.,
588 Ohkubo, T., Samper, C., Sukumar, R., Sun, I.-F., Nur Supardi, M. N., Tan, S., Thomas, D., Thompson, J.,
589 Valencia, R., Vallejo, M. I., Munoz, G. V., Yamakura, T., Zimmerman, J. K., Dattaraja, H. S., Esufali, S.,
590 Hall, P., He, F., Hernandez, C., Kiratiprayoon, S., Suresh, H. S., Wills, C., and Ashton, P.: Comparing
591 tropical forest tree size distributions with the predictions of metabolic ecology and equilibrium models,
592 *Ecol Letters*, 9, 589–602, <https://doi.org/10.1111/j.1461-0248.2006.00915.x>, 2006a.

593 Muller-Landau, H. C., Condit, R. S., Chave, J., Thomas, S. C., Bohlman, S. A., Bunyavejchewin, S.,
594 Davies, S., Foster, R., Gunatilleke, S., Gunatilleke, N., Harms, K. E., Hart, T., Hubbell, S. P., Itoh, A.,
595 Kassim, A. R., LaFrankie, J. V., Lee, H. S., Losos, E., Makana, J.-R., Ohkubo, T., Sukumar, R., Sun, I.-F.,
596 Nur Supardi, M. N., Tan, S., Thompson, J., Valencia, R., Munoz, G. V., Wills, C., Yamakura, T., Chuyong,
597 G., Dattaraja, H. S., Esufali, S., Hall, P., Hernandez, C., Kenfack, D., Kiratiprayoon, S., Suresh, H. S.,
598 Thomas, D., Vallejo, M. I., and Ashton, P.: Testing metabolic ecology theory for allometric scaling of tree
599 size, growth and mortality in tropical forests, *Ecol Letters*, 9, 575–588, [https://doi.org/10.1111/j.1461-](https://doi.org/10.1111/j.1461-0248.2006.00904.x)
600 [0248.2006.00904.x](https://doi.org/10.1111/j.1461-0248.2006.00904.x), 2006b.

601 Muller-Landau, H. C., Cushman, K. C., Arroyo, E. E., Martinez Cano, I., Anderson-Teixeira, K. J., and
602 Backiel, B.: Patterns and mechanisms of spatial variation in tropical forest productivity, woody residence
603 time, and biomass, *New Phytol*, 229, 3065–3087, <https://doi.org/10.1111/nph.17084>, 2021.

604 Negrón-Juárez, R. I., Chambers, J. Q., Guimaraes, G., Zeng, H., Raupp, C. F. M., Marra, D. M., Ribeiro, G.
605 H. P. M., Saatchi, S. S., Nelson, B. W., and Higuchi, N.: Widespread Amazon forest tree mortality from a
606 single cross-basin squall line event: WIND-DRIVEN TREE MORTALITY IN AMAZONIA, *Geophys.*
607 *Res. Lett.*, 37, n/a-n/a, <https://doi.org/10.1029/2010GL043733>, 2010.

608 Negrón-Juárez, R. I., Jenkins, H. S., Raupp, C. F. M., Riley, W. J., Kueppers, L. M., and Marra, D. M.:
609 Windthrow Variability in Central Amazonia, 17, 2017.

610 Negrón-Juárez, R. I., Holm, J. A., Marra, D. M., Rifai, S. W., Riley, W. J., Chambers, J. Q., Koven, C. D.,
611 Knox, R. G., McGroddy, M. E., Di Vittorio, A. V., Urquiza-Muñoz, J., Tello-Espinoza, R., Muñoz, W. A.,
612 Ribeiro, G. H. P. M., and Higuchi, N.: Vulnerability of Amazon forests to storm-driven tree mortality,
613 *Environ. Res. Lett.*, 13, 054021, <https://doi.org/10.1088/1748-9326/aabe9f>, 2018.

614 Phillips, O. L., Lloyd, J., Malhi, Y., Monteagudo, A., Almeida, S., Davila, E. A., Amaral, I., Andelman, S.,
615 Andrade, A., Arroyo, L., Aymard, G., Baker, T. R., and Bonal, D.: Drought–mortality relationships for
616 tropical forests, 16, 2010.

617 Silva, C. A., Valbuena, R., Pinagé, E. R., Mohan, M., Almeida, D. R. A., North Broadbent, E., Jaafar, W.
618 S. W. M., Papa, D., Cardil, A., and Klauberger, C.: ForestGapR: An r Package for forest gap analysis from
619 canopy height models, *Methods Ecol Evol*, 10, 1347–1356, <https://doi.org/10.1111/2041-210X.13211>,
620 2019.

621 Silva, C. V. J., Aragão, L. E. O. C., Barlow, J., Espirito-Santo, F., Young, P. J., Anderson, L. O.,
622 Berenguer, E., Brasil, I., Foster Brown, I., Castro, B., Farias, R., Ferreira, J., França, F., Graça, P. M. L. A.,
623 Kirsten, L., Lopes, A. P., Salimon, C., Scaranello, M. A., Seixas, M., Souza, F. C., and Xaud, H. A. M.:
624 Drought-induced Amazonian wildfires instigate a decadal-scale disruption of forest carbon dynamics, *Phil.*
625 *Trans. R. Soc. B*, 373, 20180043, <https://doi.org/10.1098/rstb.2018.0043>, 2018.

626 Solé, R. V. and Manrubia, S. C.: Are rainforests self-organized in a critical state?, *Journal of Theoretical*
627 *Biology*, 173, 31–40, <https://doi.org/10.1006/jtbi.1995.0040>, 1995.

628 Windsor, D. M.: Climate and moisture variability in a tropical forest: long- term records from Barro
629 Colorado Island, Panamá, *Smithsonian Contributions to the Earth Sciences*, 29, 1–45,
630 <https://doi.org/10.5479/si.00810274.29.1>, 1990.

631 Xu, L., Saatchi, S. S., Yang, Y., Yu, Y., Pongratz, J., Bloom, A. A., Bowman, K., Worden, J., Liu, J., Yin,
632 Y., Domke, G., McRoberts, R. E., Woodall, C., Nabuurs, G.-J., de-Miguel, S., Keller, M., Harris, N.,
633 Maxwell, S., and Schimel, D.: Changes in global terrestrial live biomass over the 21st century, *Sci. Adv.*, 7,
634 eabe9829, <https://doi.org/10.1126/sciadv.abe9829>, 2021.

635 Yanoviak, S. P., Gora, E. M., Burchfield, J. M., Bitzer, P. M., and Detto, M.: Quantification and
636 identification of lightning damage in tropical forests, *Ecol Evol*, 7, 5111–5122,
637 <https://doi.org/10.1002/ece3.3095>, 2017.

638 Zahawi, R. A., Dandois, J. P., Holl, K. D., Nadwodny, D., Reid, J. L., and Ellis, E. C.: Using lightweight
639 unmanned aerial vehicles to monitor tropical forest recovery, *Biological Conservation*, 186, 287–295,
640 <https://doi.org/10.1016/j.biocon.2015.03.031>, 2015.

641